High-field (3 Tesla) MRI of the navicular apparatus of sound horses shows good agreement to histopathology

Kottmeier, Lena K ; Seehusen, Frauke ; Helweg, Martin ; Rohn, Karl ; Stadler, Peter ; Hellige, Maren

Abstract: Magnetic resonance imaging and the correlation to histopathological findings of the equine palmar foot of lame horses have been described previously, using 0.27 and 1.5 T systems. Compared to these, 3 T systems provide superior spatial resolution and imaging contrast. The aim of our prospective anatomic study was to characterize the imaging anatomy of the navicular region on 3 T MRI in comparison to histopathological findings. We hypothesized that 3 T MRI allows a good visualization of the entire navicular apparatus and reliable measurements of navicular cartilage and cortical bone thickness. Twenty front feet of sound horses were examined using a 3 T MRI system. For histopathological examination, sagittal tissue sections of the navicular bones and adjacent ligaments were prepared. Alterations in magnetic resonance signal were graded for each region and compared to corresponding histological slices. Overall, there was good visualization of the anatomical detail and a very good agreement between MRI and histology for compact bone and spongiosa, good agreement for the fibrocartilage and the distal sesamoidean impar ligament, but only moderate agreement for the hyaline cartilage and the collateral sesamoidean ligament. A comparative measurement of cartilage and cortical bone thickness on magnetic resonance images and histological sections was performed. In MRI, the hyaline cartilage of the articular surface appeared significantly thinner and the fibrocartilage of the flexor surface appeared significantly thicker compared to histology. Findings indicated that MRI at a field strength of 3 T allows reliable depiction of anatomic details of the navicular apparatus.

DOI: https://doi.org/10.1111/vru.12825

Originally published at:
Kottmeier, Lena K; Seehusen, Frauke; Helweg, Martin; Rohn, Karl; Stadler, Peter; Hellige, Maren (2020). High-field (3 Tesla) MRI of the navicular apparatus of sound horses shows good agreement to histopathology. Veterinary Radiology Ultrasound, 61(1):48-57.
DOI: https://doi.org/10.1111/vru.12825

Received: 28 April 2019 | Revised: 9 September 2019 | Accepted: 12 September 2019

DOI: 10.1111/vru.12825

WILEY

ORIGINAL INVESTIGATION

High-field (3 Tesla) MRI of the navicular apparatus of sound horses shows good agreement to histopathology

Lena K. Kottmeier[1] | Frauke Seehusen[2] | Martin Helweg[1] | Karl Rohn[3] | Peter Stadler[1] | Maren Hellige[1]

[1]Clinic for Horses, University of Veterinary Medicine Hannover, Foundation, Hannover, Germany

[2]Department of Pathology, University of Veterinary Medicine Hannover, Foundation, Hannover, Germany

[3]Institute for Biometry, Epidemiology, and Information Processing, University of Veterinary Medicine Hannover, Foundation, Hannover, Germany

Correspondence
Maren Hellige, Clinic for Horses, University of Veterinary Medicine Hannover, Foundation, Bünteweg 9, Hannover 30559, Germany.
Email: maren.hellige@tiho-hannover.de

Abstract

Magnetic resonance imaging and the correlation to histopathological findings of the equine palmar foot of lame horses have been described previously, using 0.27 and 1.5 T systems. Compared to these, 3 T systems provide superior spatial resolution and imaging contrast. The aim of our prospective anatomic study was to characterize the imaging anatomy of the navicular region on 3 T MRI in comparison to histopathological findings. We hypothesized that 3 T MRI allows a good visualization of the entire navicular apparatus and reliable measurements of navicular cartilage and cortical bone thickness. Twenty front feet of sound horses were examined using a 3 T MRI system. For histopathological examination, sagittal tissue sections of the navicular bones and adjacent ligaments were prepared. Alterations in magnetic resonance signal were graded for each region and compared to corresponding histological slices. Overall, there was good visualization of the anatomical detail and a very good agreement between MRI and histology for compact bone and spongiosa, good agreement for the fibrocartilage and the distal sesamoidean impar ligament, but only moderate agreement for the hyaline cartilage and the collateral sesamoidean ligament. A comparative measurement of cartilage and cortical bone thickness on magnetic resonance images and histological sections was performed. In MRI, the hyaline cartilage of the articular surface appeared significantly thinner and the fibrocartilage of the flexor surface appeared significantly thicker compared to histology. Findings indicated that MRI at a field strength of 3 T allows reliable depiction of anatomic details of the navicular apparatus.

KEYWORDS

high-field MRI, histology, horse, navicular bone

1 | INTRODUCTION

Magnetic resonance imaging has become an important diagnostic tool to investigate the source of lameness in the distal limb. Injuries of the navicular apparatus are a common finding in horses diagnosed with foot pain.[1,2] A comparison of MRI and histopathology in the palmar foot has previously been described using low-field (0.27 T) and high-field (1.5 T) MRI systems.[2–7] Agreement of 1.5 T MRI and histologic examination for tissue grading was very good for the navicular bursa and good for the spongiosa of the navicular bone and the collateral sesamoidean ligament.[7] Agreement between the appearance on MRI and histology was described as moderate to good for the palmar and distal aspects of the navicular bone, but only fair to moderate for the distal sesamoidean impar ligament and poor for the dorsal and proximal aspects of the navicular bone.[2,7] In particular, the articular surface of the navicular bone is susceptible to artifacts and was not clearly visible when using 1.5 T MRI.[7]

Signal irregularities associated with artifacts are not uncommon in MRI and have to be distinguished from signal irregularities caused by tissue damage.[8,12] In our study, a 3 T scanner was used. In general, a

Previous publication or presentation disclosure: Presented as an abstract at National Scientific Meeting (DVG Pferdekrankheiten – German Veterinary Association, Equine Medicine) in 2012.

EQUATOR network disclosure: EQUATOR network checklist was not used.

TABLE 1 Parameters used in pulse sequences for imaging horse's limbs with a 3-Tesla MRI system

Pulse sequence	Plane	TE (ms)	TR (ms)	Slice thickness (mm)	Interslice gap (mm)	Field of view (mm)	Reconstructed matrix
Proton density high resolution	Sagittal	30	2034	3	0.3	200 × 98	1024 × 1024
T1	Sagittal	19	668	3	0.3	200 × 98	1024 × 1024
Proton density Spectral Attenuated Inversion Recovery	Sagittal	30	2853	3	0.3	200 × 98	720 × 720
Proton density high resolution	Transverse	30	1107	3	0.3	100 × 100	512 × 512
T1	Transverse	19	500	3	0.3	100 × 100	512 × 512
Proton density Spectral Attenuated Inversion Recovery	Transverse	30	1298	3	0.3	100 × 100	512 × 512
Proton density high resolution	Dorsal	16	1911	3	0.3	150 × 100	1024 × 1024

higher magnetic field strength provides an increase in the signal-to-noise ratio that allows increased spatial resolution.[9,10] An early indicator of navicular disease is thinning of the fibrocartilage, which is challenging to diagnose with any diagnostic modality.[4,11–13] Identification of fibrocartilage loss could serve earlier and more successful therapeutic intervention. To date, the compared measurements of cartilage produced variable results in human and veterinary medicine. Several studies have underestimated articular cartilage thickness in comparison to histology,[14–16] but overestimated the thickness of the navicular fibrocartilage using 1.5 T MRI.[13] There has been no description of the navicular apparatus using 3 T MRI so far and it is not known how accurate MRI reflects dimensions of navicular cartilage and bone. The aim of our study was to describe the navicular region of clinically sound horses as it appears on 3 T MRI and compare it to histopathological results. We hypothesized that 3 T MRI allows a good visualization of all aspects of the navicular apparatus, including the articular surface and the proximal border of the navicular bone and that 3 T MRI would allow reliable measurements of subchondral bone, hyaline cartilage, fibrocartilage, and compact bone.

2 | METHODS

The study was a prospective, anatomic design. Ten horses (nine Warmbloods and one Standardbred) with a mean age of 6.5 years (range 4-20 years) and with a mean bodyweight of 550 kg (range 482-620 kg) were included. Institutional Animal Care and Use Committee approval had been granted for the combined prospective study of these research horses.* Prior to MRI examination, all horses underwent a complete clinical examination and lameness workup performed by an experienced equine surgeon. Thus, horses were excluded if a lameness of the thoracic limbs was present in a 4 months period prior to the study or if they responded positive to the flexion test of the front limbs prior to the MRI examination. All decisions for subject inclusion or exclusion were made by the last author, an experienced equine surgeon. Subsequent to MRI, all horses were humanely destroyed for reasons unrelated to this study.

2.1 | MRI

Horses underwent general anesthesia and were positioned in lateral recumbency. An eight-channel SENSE phased-array receive coil (SENSE knee coil, Philips International B.V., Amsterdam, The Netherlands) was positioned at the foot and magnetic resonance images were acquired using a 3 T MRI system (Philips Achieva 3.0 T, Philips International B.V.). Sequences were obtained in sagittal, transverse, and dorsal planes. Sequences used were proton density high resolution, T1 turbo spin echo, and proton density with fat saturation (spectral attenuated inversion recovery) (Table 1). Image acquisition took approximately 30 min per foot and both front feet were examined.

2.2 | Image interpretation

The magnetic resonance images of the 20 front feet were reviewed using a diagnostic workstation (easyIMAGE, VetZ, Isernhagen, Germany) in a randomized order by three observers independently (two trained interns and one experienced equine surgeon) using a grading system established for evaluation of the navicular bone in high-field (1.5 T) magnetic resonance images.[8] The observers were not aware of the histopathological findings at the time of data recording. The navicular apparatus including the navicular bone, the adjacent ligaments, and the navicular bursa was divided in eight regions: proximal margin, distal margin, articular surface, flexor surface and spongiosa of the navicular bone, the navicular bursa and the distal sesamoidean impar ligament, and the axial collateral sesamoidean ligament. For each anatomical region, alterations in signal intensity and homogeneity and the definition of anatomic margins were scored from 0 (no changes) to 3 (severe abnormalities). The maximal score per slice from all observers was taken as magnetic resonance grading for this structure and compared to histological grading via a two-dimensional

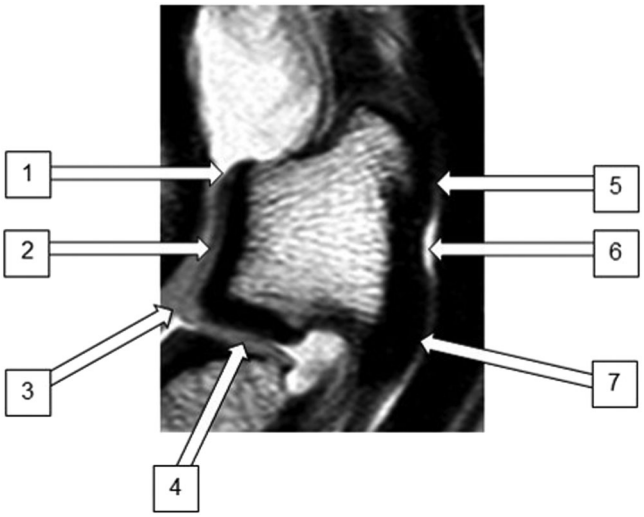

FIGURE 1 Measuring points on the navicular bone shown on a mid-sagittal proton density-weighted image (TE, 30 ms; TR, 2034 ms; slice thickness, 3 mm). 1, dorsoproximal edge of the navicular bone; 2, mid articular surface of the navicular bone: 3, dorsodistal edge of the navicular bone; 4, distal border of the navicular bone; 5, palmaroproximal region of the navicular bone; 6, central flexor surface of the navicular bone; 7, palmarodistal region of the navicular bone

contingency table to display the frequency distribution of the variables.

Measurements of the hyaline cartilage at the articular surface, the fibrocartilage at the flexor surface, and the compact bone of the articular and flexor surface were applied on three midsagittal magnetic resonance scans in proton density-weighted, T1-weighted, and proton density with fat saturation (spectral attenuated inversion recovery)-weighted sequences. Seven measuring points were set at the navicular bone: proximal, central, and distal both on the articular and the flexor surface, respectively, and at the distal margin (Figure 1). All measurements were taken perpendicular to the cartilage surface.

2.3 | Tissue harvest

The navicular bones of the front feet and their supporting ligaments were dissected. The samples were fixed in 10% buffered formalin, cut into sagittal slices with a thickness of 3 mm, decalcified for 4 weeks, and subsequently embedded in paraffin wax and sectioned at 3 μm. From every 3-mm tissue sample, three slides were stained with hematoxylin and eosin (Figure 2) as described in standard laboratory procedures.[17]

2.4 | Histopathologic examination

All sagittal sections (40-51 per navicular bone) were graded by a trained equine intern and an European College of Veterinary Pathology certified pathologist in consensus. The observers were not aware of the MRI findings at the time of data recording. The above described eight anatomical regions were evaluated by light microscopy (100× magnification), applying an established, slightly modified scoring system.[1] The examination included proximal and

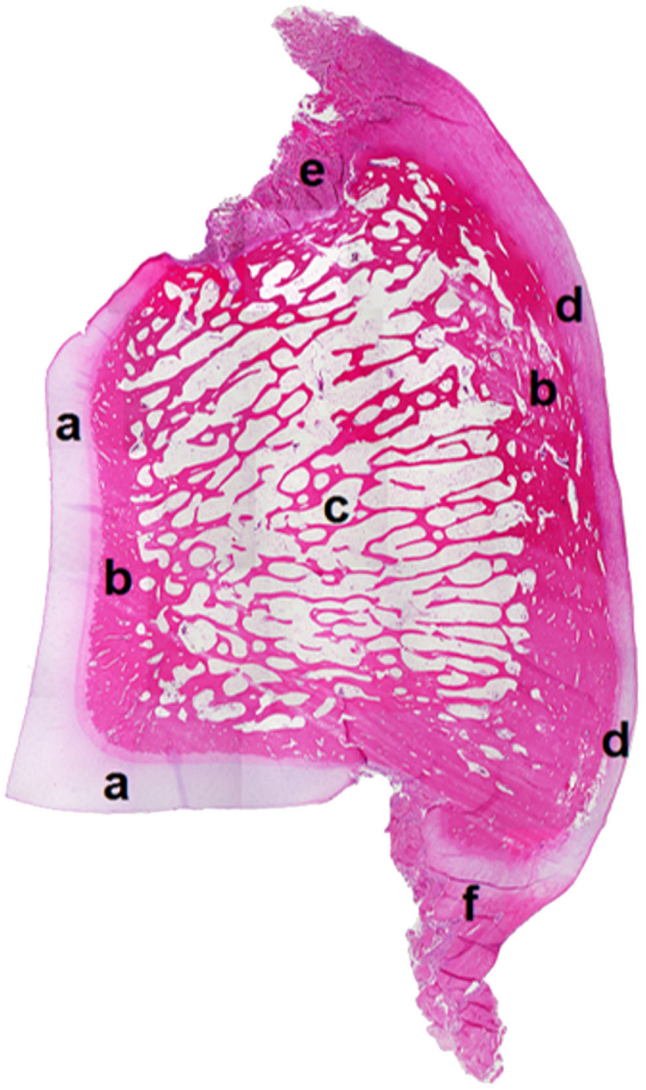

FIGURE 2 Sagittal tissue section of a navicular bone. Hematoxylin and eosin stain; a, hyaline cartilage; b, compact bone; c, spongiosa; d, fibrocartilage; e, insertion of the axial collateral sesamoidean ligament; f, origin of the distal sesamoidean impar ligament [Color figure can be viewed at wileyonlinelibrary.com]

distal margins, articular and flexor surfaces, spongiosa and origin of the distal sesamoidean impar ligament as well as the insertion of the axial collateral sesamoidean ligament. The severity of histological findings for each site was scored from 0 (no changes) to 3 (severe abnormalities). Histopathologic changes in cartilage were characterized as reduction in depth, fibrillation, and erosion, loss of cellularity, chondrocyte response, chondrocyte formation, and irregular tidemark. Criteria for bone changes were microfractures, myelofibrosis, widening of the intertrabecular spaces, cyst-like lesions, hemosiderin, hemosiderophages, inflammatory cells, and accumulation of osteoclasts. The proximal and distal margins with the distal sesamoidean impar ligament and axial collateral sesamoidean ligament attached were examined for signs of fibrocartilaginous metaplasia, accumulation of osteoclasts and inflammatory cells, enthesophytes, osteonecrosis, and enlarged synovial invaginations.

Each tissue section was photographed with a camera-microscope combination and measurements of cortical bone thickness and cartilage thickness were taken using an imaging software (cell D, Olympus, Hamburg, Germany). Seven measuring points corresponding to the magnetic resonance images were set at the navicular bone: proximal, central, and distal both on articular surface and the flexor surface, respectively, and at the distal margin (Figure 1). All measurements were taken perpendicular to the cartilage surface, once with and once without consideration of the tidemark.

2.5 | Statistics

Selection and completion of the statistical tests was performed by a professional biostatistician. McNemar's test of symmetry and the kappa (κ) statistic were used to test agreement between histopathology and MRI scoring. The relative strength of agreement was interpreted as follows: kappa values ≤0.2 demonstrates poor agreement, 0.21-0.4 fair agreement, 0.41-0.6 moderate agreement, 0.61-0.8 good agreement, and ≥0.81 very good agreement.[18] A multi factor analysis of variance and a *t*-test were used to test for an association between measurements obtained with MRI and histomorphometrically and between different MRI sequences. A value of $P < .05$ was considered significant. Data analysis was performed with the statistics program package (SAS®, Version 9.3, SAS Institute, Cary, NC, USA).

3 | RESULTS

3.1 | Flexor surface

In all images, the flexor surface was clearly separated from the hyperintense signal of the synovial fluid of the navicular bursa on proton density and proton density with fat saturation (spectral attenuated inversion recovery)-weighted sequences and the hypointense signal of the deep digital flexor tendon. Fibrocartilage and synovial fluid were not distinguishable on every magnetic resonance image. The fibrocartilage was graded as normal if it was seen as a clear layer over the entire surface and was determined as degenerative if irregularities or loss of signal definition was seen.[8] In nine cases (45%), the fibrocartilage was graded normal both in MRI and histology; in eight cases (40%), the fibrocartilage was consistently evaluated as mildly degenerated (grade 1); and in three cases (15%), the fibrocartilage was mildly degenerated histologically (grade 1) but inconspicuous on MRI (grade 0). There was good agreement ($\kappa = .70$) between MRI and histology for the fibrocartilage.

The palmar cortex was graded normal in 17 cases (85%) in MRI and histology. One horse exhibited accumulation of osteoclasts and myelofibrosis in the palmar cortex, bilaterally (histology grade 1), and a slightly irregular interface between spongiosa and cortical bone in MRI (grade 1). One navicular bone sustained grade 1 signal alterations in MRI but was inconspicuous by means of histopathology. In comparison, there was good agreement of the flexor cortex bone ($\kappa = .77$).

3.2 | Articular surface

The hyaline cartilage at the articular surface of the navicular bone was well demarcated from the hypointense signal of the dorsal cortex and the synovial fluid of the distal interphalangeal joint in proton density and proton density with fat saturation (spectral attenuated inversion recovery)-weighted sequences. In seven navicular bones (35%), there was a loss of definition of the outline of the articular surface in some sagittal planes, regardless of the magnetic resonance sequence. The hyaline cartilage showed remarkable variations in shape of the dorsoproximal border. Some navicular bones presented with a smooth outlining (Figure 3A), others with an irregular outlining (Figure 3B-C). The corresponding histological presentation of these findings revealed either a wavy-shaped cartilage or single thin fibers of the axial collateral sesamoidean ligament that overlaid the cartilaginous tissue (Figure 3D-E). The hyaline cartilage itself was of heterogeneous signal intensity in all MRI sequences, with a typical pattern recognition: at the proximal part of the articular surface, as well as at the distal margin, a decreased signal intensity appears. The middle aspect of the cartilage was of medium signal intensity, with a focal oval-shaped area of increased signal next to the dorsal edge. Consequently, it was possible to differentiate five areas within the hyaline cartilage (Figure 4). Three navicular bones (15%) sustained grade 1 erosions of the hyaline cartilage on histology, which were not apparent on magnetic resonance images (grade 0). Two navicular bones (10%) sustained grade 1 erosions (indentations of approximately 0.3 mm depth) in the cartilage, which were all detectable on magnetic resonance images (grade 1). All other navicular bones (75%) did not show any lesions at the hyaline cartilage and were graded as normal (grade 0) in histology and MRI. In conclusion, agreement between grading in MRI and histology for the hyaline cartilage was moderate ($\kappa = .5$).

The cortex at the articular surface appeared normal (grade 0) on MRI in all but two navicular bones (90%), in which a slightly irregular tidemark was identified (grade 1) but no histopathologic changes were present. Thus, agreement in grading was very good ($\kappa = .8$).

3.3 | Spongiosa

The spongiosa showed homogenous hypointense signal in fat-suppressed proton density with fat saturation (spectral attenuated inversion recovery)-weighted images and intermediate to hyperintense signal in proton density and T1 weighted sequences without any signal alterations (grade 0). Correspondingly, no histopathological findings were recorded within the spongiosa (grade 0). The agreement between grading in MRI and histology was very good ($\kappa = 1$).

3.4 | Proximal margin and collateral sesamoidean ligament

The proximal compact bone was of uniform low signal intensity. In three navicular bones (15%), grade 1 irregularities were evident on MRI and histology. There was very good agreement between MRI and histology ($\kappa = 1$).

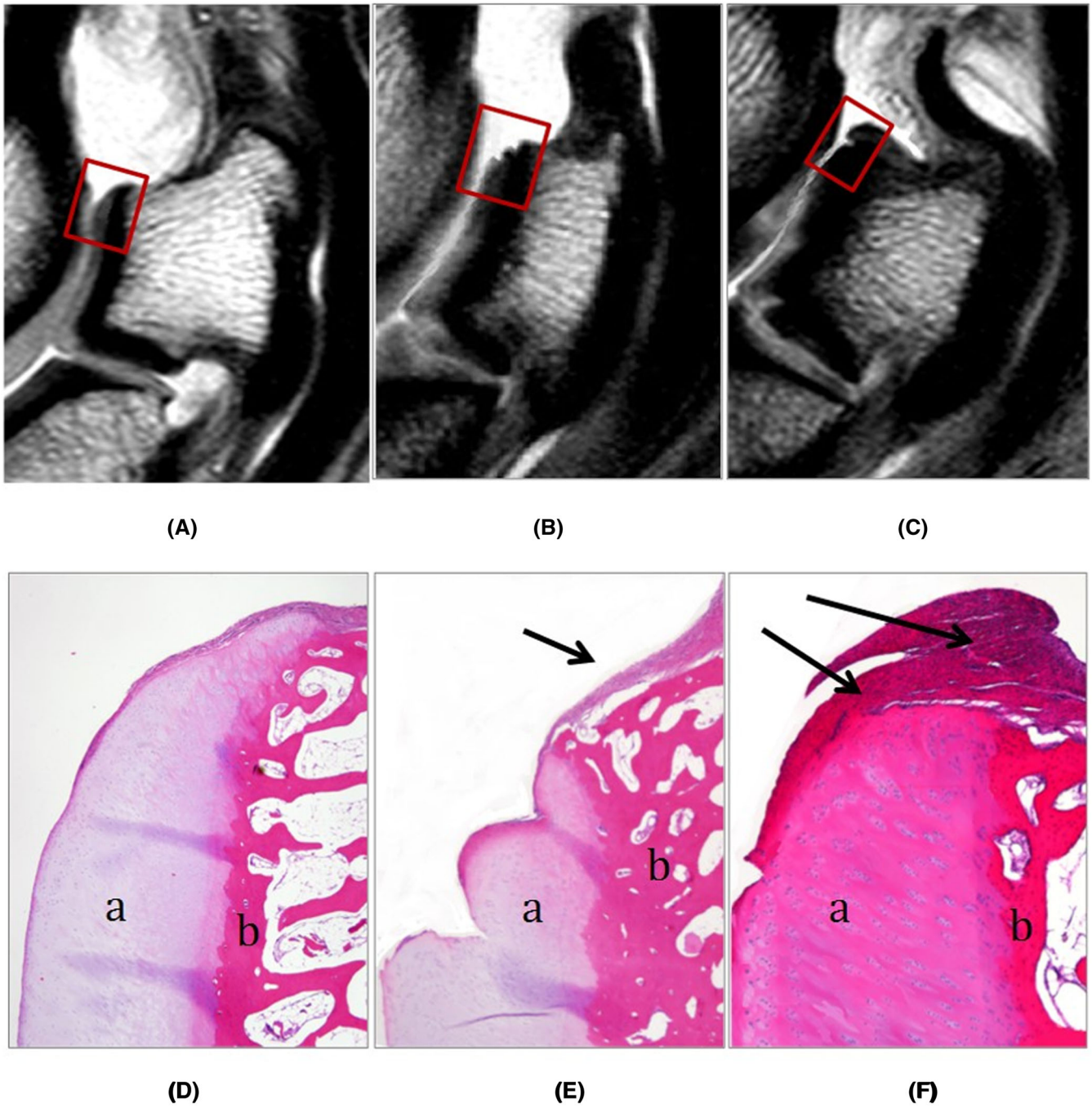

FIGURE 3 Appearance of various formations of the proximal aspect of the articular surface; comparison of 3-T MRI (A-C, sagittal plane, proton density-weighted sequence) and histology (Hematoxylin and eosin stain, D-F). A and D, Regular and smooth hyaline cartilage; B and E, uneven outline of the hyaline cartilage; C and F, hyaline cartilage overlies with fibers of the axial collateral sesamoidean ligament; a, hyaline cartilage; b, compact bone; arrow, fibers of the axial collateral sesamoidean ligament [Color figure can be viewed at wileyonlinelibrary.com]

The axial collateral sesamoidean ligament showed low signal intensity in all sequences. However, in all sagittal slices of all navicular bones there was a region of increased signal intensity at the insertion of the collateral sesamoidean ligament (Figure 5). Histologically, the collateral sesamoidean ligament showed mainly cross-sectioned collagen fibers, connective tissue, and individual vessels in this region, but no lesions were detected. Agreement between MRI and histology was moderate ($\kappa = .57$).

3.5 | Distal margin and distal sesamoidean impar ligament

There were no pathologic changes at the distal cortex in 16 limbs (80%). There were four navicular bones with grade 1 irregularities in histology; two of them were graded normal on MRI (grade 0). Agreement between MRI and histology for the distal compact bone was good ($\kappa = .61$).

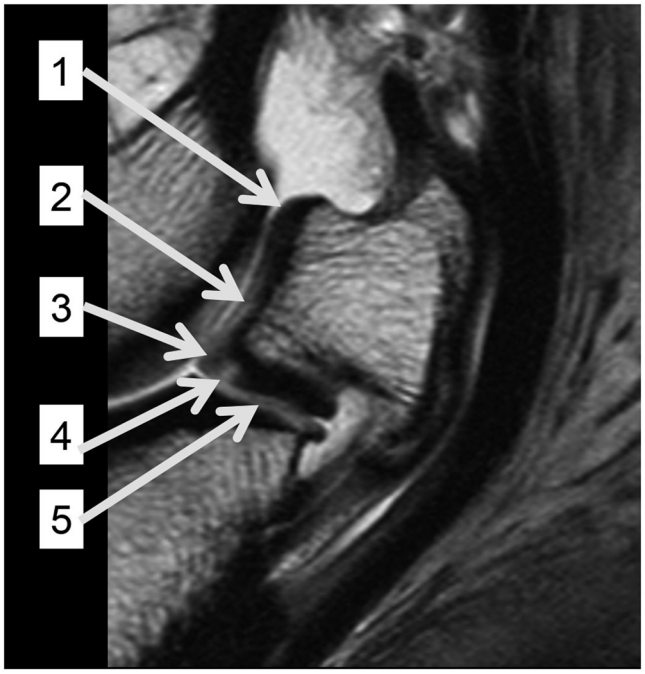

FIGURE 4 Magnetic resonance signal pattern in hyaline cartilage of the navicular bone (sagittal proton density-weighted image (TE, 30 ms; TR, 2034 ms; slice thickness, 3 mm); 1, hypointense signal proximal at the articular surface; 2, hyperintense signal centrally and distally; 3, intermediate signal at the distal edge of the articular surface; 4, intermediate signal next to the dorsal edge of the distal border; 5, hypointense signal at the distal border. This signal pattern was common at the hyaline cartilage and may be related to partial volume averaging

The distal sesamoidean impar ligament appeared slightly striated and could be distinguished easily from the hyperintense signal of the navicular bursa and the distal interphalangeal joint. In 14 navicular bones (70%), there was no evidence of any abnormalities at the origin of the distal sesamoidean impar ligament, neither in MRI nor in histology (grade 0). One case was consistently rated as grade 1 (5%). Two navicular bones (10%) had isolated osseous fragments within the distal sesamoidean impar ligament (grade 3), both were obvious on MRI (grade 3, Figure 6). The fragments were surrounded by an area of fibrocartilaginous metaplasia and chondroid tissue. Additionally, an accumulation of inflammatory cells and osteoclasts was evident. Three ligaments (15%) were graded as normal in MRI (grade 0) but showed grade 1 alterations by means of histology. The agreement in grading between methods was good ($\kappa = .61$).

4 | RESULTS OF MEASUREMENTS

4.1 | Hyaline cartilage

In all navicular bones, the hyaline cartilage appeared significantly thinner on MRI compared to histology (see Table 2). After excluding the calcified cartilage (mean thickness 0.3 mm) from the histological measurement, there was no more significant difference between measurements ($P = .06$).

FIGURE 5 Sagittal plane (proton density weighted) mildly increased signal intensity at the insertion of the axial collateral sesamoidean ligament (collateral sesamoidean ligament, arrow)

4.2 | Fibrocartilage

At the proximal aspect of the flexor surface, the fibrocartilage appeared significantly thinner on MRI compared to histology ($P < .001$). In contrast, in the central region of the flexor surface, the fibrocartilage was significantly thicker on MRI, compared to histology ($P < .001$). At the distal measuring point, there was no significant difference between results of MRI and histology ($P = .52$; see Table 2, measuring point 5-7). The magnetic resonance sequences did affect the measuring of the fibrocartilage. In proton density with fat saturation (spectral attenuated inversion recovery)-weighted images, the fibrocartilage came out significantly thicker compared to proton density or T1-weighted images ($P = .007$).

4.3 | Compact bone

There was good agreement between measurements of the compact bone at the articular surface. There was neither a significant difference between measurements at the proximal measuring point ($p = 0.2$), at the central ($p = 0.4$) nor the distal measuring point ($p = 0.4$). But we recognized a slightly overestimation of bone thickness distal at the articulation site with the distal phalanx in MRI, compared to histology, but with slight significance ($p = 0.02$).

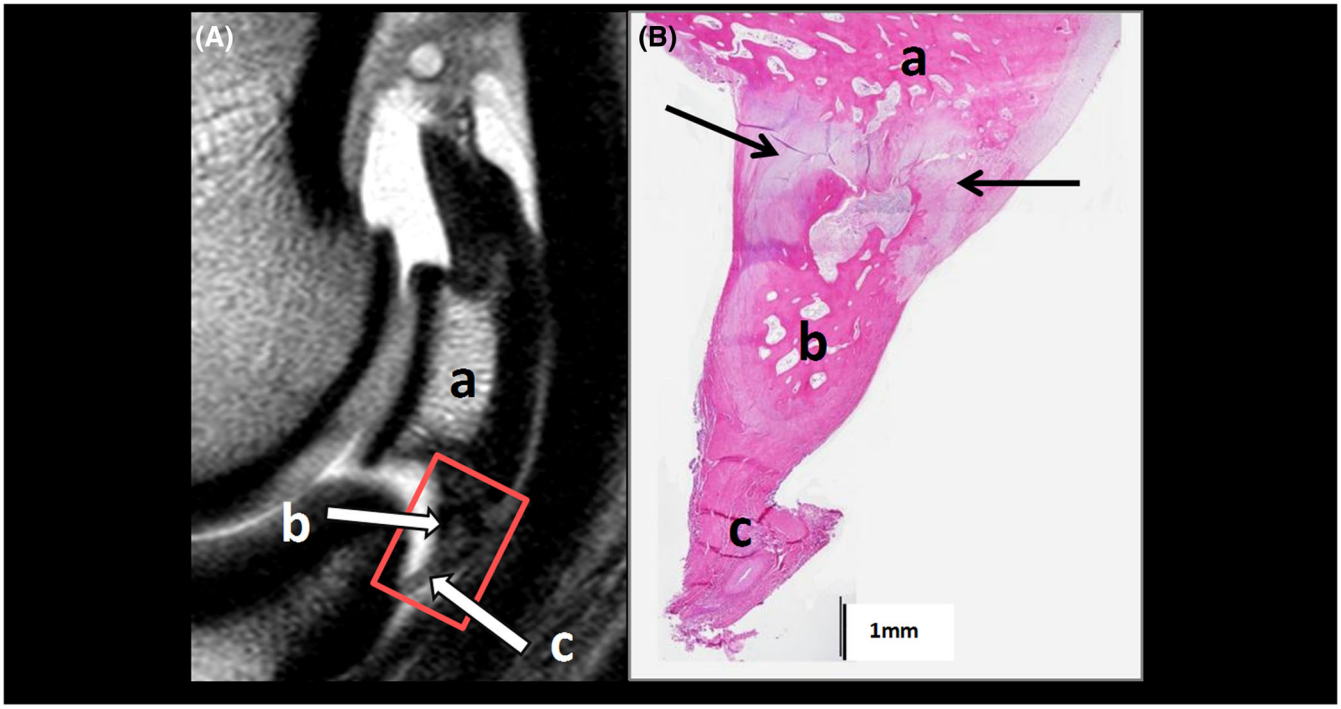

FIGURE 6 Distal border fragment in the distal sesamoidean impar ligament. A, Bone fragment (b, arrow) on sagittal magnetic resonance image (proton density weighted; slice thickness, 3 mm); c, arrow: distal aspect of the distal sesamoidean impar ligament. B, Same bone fragment in tissue section (hematoxylin and eosin stain). There is an area of basophil cartilage (arrows) between the bone fragment (b) and the distal border of the navicular bone (a); a, navicular bone; b, distal border fragment; c, distal sesamoidean impar ligament [Color figure can be viewed at wileyonlinelibrary.com]

TABLE 2 Thickness of the cartilage and compact bone in MRI compared to histology on different measuring points, including the calcified cartilage, that is only visible in the histology images (1-7, Figure 1)

Measuring point (s. Figure 1)	Structure	Thickness MRI (mm)	Thickness histology (mm)	*P*-value
1	Hyaline cartilage	0.7 ± 0.2	1.3 ± 0.3	<.001*
	Compact bone	1.3 ± 0.5	1.3 ± 0.5	.2
2	Hyaline cartilage	1.0 ± 0.2	1.4 ± 0.3	<.001*
	Compact bone	1.4 ± 0.5	1.4 ± 0.5	.4
3	Hyaline cartilage	1.9 ± 0.4	2.5 ± 0.5	<.001*
	Compact bone	1.4 ± 0.5	2.5 ± 1	<.001*
4	Hyaline cartilage	1.0 ± 0.3	1.4 ± 0.3	<.001*
	Compact bone	1.5 ± 0.4	1.3 ± 0.6	.02
5	Fibrocartilage	0.3 ± 0.2	1.0 ± 0.3	<.001*
	Compact bone	1.8 ± 0.8	1.7 ± 0.6	.02
6	Fibrocartilage	1.0 ± 0.3	0.8 ± 0.2	<.001*
	Compact bone	2.2 ± 0.8	1.8 ± 0.6	<.001*
7	Fibrocartilage	0.6 ± 0.3	0.6 ± 0.1	.52
	Compact bone	2.8 ± 0.8	2.3 ± 0.5	<.001*

*Statistically significant difference.

In contrast, there was a significant difference between measurements at the palmar cortex. The cortex appeared significantly thicker in MRI, compared to histology ($p = 0.02$) for the proximal measuring point, and $p < 0.001$ for the central, as well as at the distal measuring point.

5 | DISCUSSION

The results of this study supported the hypothesis that 3 T MRI allows good visualization of anatomic details in the equine navicular apparatus. Poor agreement between 1.5 T MRI and histological

grading has been reported for the dorsal and proximal border of the navicular bone.[7] In the present study, the agreement in grading at the articular surface was better than postulated for 1.5 T MRI (moderate agreement for the hyaline cartilage; very good agreement for the dorsal compact bone). This can be explained by the fact that a higher field strength results in a lower signal-to-noise ratio, increased spatial resolution, and decreased susceptibility to artifacts.[9,10] In our study, 3 T MRI provided detailed information about the signal distribution within the hyaline cartilage of the articular surface that previous studies failed to resolve.[7] However, a loss of the definition of the articular surface of the navicular bone was seen on some sagittal slices in MRI. This signal change is, most likely, caused by the partial volume averaging artifact. The artifact occurs, when tissues of different signal intensity are encompassed on the same voxel possessing a signal average of both tissues. Although the articular surface of the navicular bone is usually not the focus of equine clinicians, it is known that 65-75% of horses do have focal lesions at this location[1] and false positive results can occur during image interpretation.[7]

Several horses showed a focal hyperintense signal in the fibrocartilage layer due to pooling of synovial fluid next to the sagittal ridge—obvious in proton density and proton density with fat saturation (spectral attenuated inversion recovery)-weighted sequences. This finding was likely due to the mid-ridge synovial fossa (*fossa nudata)*, which is considered a normal anatomical variation.[13,20]

Alterations at the proximal border of the navicular bone have been over interpreted on 1.5 T magnetic resonance images compared to histology.[7] The agreement between MRI grading and histological grading at the proximal border was very good ($\kappa = 1$) in our study, but mild pathological changes were evident.

The axial collateral sesamoidean ligament was formerly described as structure of homogeneous low signal intensity on spoiled gradient echo and gradient echo sequences, interspersed with uniformly distributed areas of higher signal on gradient echo.[8] In contrast, we described a generally increased signal at the insertion in sagittal slices (Figure 5) in our group of horses without lameness. Probable explanation is the presence of mostly cross-sectioned fiber bundles in this region, compared to the rest of the ligament, as this was obvious also on histology. This might explain the increased signal intensity in all sequences in the absence of any pathological findings. Based on these results, we recommend modifying the evaluation criteria for the axial collateral sesamoidean ligament, and to consider a slightly increased signal as a physiological variation without clinical significance.

Pathologies of the distal sesamoidean impar ligament have been rated difficult to detect due to the heterogeneous appearance of the ligament.[2,7,12] In the current study, blood vessels and synovial invaginations often led to focal, clearly demarcated signal increase within the distal sesamoidean impar ligament and should not be misinterpreted as pathological findings. Two navicular bones had a distal border fragment, which appeared as an oval-shaped area of low signal intensity within the distal sesamoidean impar ligament. Agreement between MRI and histological grading for the distal sesamoidean impar ligament was good ($\kappa = .61$) and therefore better than the postulated fair to moderate agreement described previously for 1.5 T images.[7] Our study supports the previously described finding of distal border fragments in nonlame horses.[19]

Another focus of this study was the correlation between measurements of bone and cartilage thickness compared to histological measurements. There is clinical interest in identifying cartilage loss at an early stage, because degeneration of the fibrocartilage is an early sign of navicular disease.[4,11–13]

Cartilage measurement at the flexor surface in this study showed good correlation in the distal half, only. This is probably related to the optimal 90° angulation of the sagittal magnetic resonance slice to the cartilage surface in the distal part. The fibrocartilage of the flexor surface is the thinnest cartilage layer in the limb, and there is no adjacent layer of synovial fluid to provide contrast due to the tight apposition between the cartilage of the flexor surface and the deep digital flexor tendon. Saline injection into the navicular bursa (magnetic resonance bursography) improved the accuracy of MRI evaluation of palmar fibrocartilage using a 1.5 T scanner.[13]

The hyaline cartilage of the articular surface turned out to be significantly thinner on MRI compared to histology. When long echo times are used, the preferential loss of signal from the deep layers of cartilage obscures the interface between cartilage and subchondral bone, which makes it difficult to obtain an accurate measurement of cartilage thickness.[13] A theory supports the hypothesis that calcified cartilage and osseous tissue have similar signal intensity and therefore will be both interpreted as subchondral bone.[14,21–23] After excluding the calcified cartilage from the measurements in our histological examination, there was no significant difference of the hyaline cartilage compared to MRI measurements anymore. However, a study on equine carpal bones determined excellent agreement of articular cartilage thickness, but only when the calcified cartilage layer was included in the measurement.[15] Probably the less curved surface of the carpal cartilage, the greater cartilage thickness, or the use of different magnetic resonance sequences compared to our study did affect the results.

The flexor cortex appeared thicker on magnetic resonance images compared to histology. Chemical shift artifacts lead to potential problems for cortical bone measurements but is limited by increasing the receive bandwidth at high-field strength.[22,23] The tendency to overestimate the bone thickness on magnetic resonance images should be kept in mind for interpreting pathological findings at the palmar border.

A limitation of the study was the relatively small number of horses without history of lameness related to the foot. Additionally, comparison between MRI and histopathology including the measurement was performed only on sagittal slice direction. The acquisition time per foot was 40 min, which is quite long and may not be practicable for every case under general anesthesia in particular when both front feet have to be examined. There was good visibility of the flexor surface on proton density and proton density with fat saturation (spectral attenuated inversion recovery)-weighted sequences but not on T1 weighted images. Therefore, it could be possible to exclude the T1 sequences in two different orientations to help save anesthesia time under clinical conditions.

In conclusion, the current study demonstrated a good visualization of anatomical details of the equine navicular apparatus using 3 T MRI under clinical conditions. Mild to severe MRI lesions were described, but the only severe lesions were distal border fragments that have been previously reported to be of no clinical significance. Care should be taken not to overinterpret mild lesions of the navicular apparatus using 3 T MRI. The agreement between MRI and histological grading was higher than previously postulated for lower field strength MRI, as we expected. The improved depiction of anatomic details in the navicular apparatus with 3 T MRI may help in understanding the spectrum of injuries that contribute to palmar foot pain and may improve future assessments of therapeutic options.

LIST OF AUTHOR CONTRIBUTIONS

Category 1

(a) Conception and Design: Kottmeier, Hellige, Stadler

(b) Acquisition of Data: Kottmeier, Hellige, Helweg, Seehusen

(c) Analysis and Interpretation of Data: Kottmeier, Hellige, Seehusen, Rohn

Category 2

(a) Drafting the Article: Kottmeier, Hellige, Helweg

(b) Revising the Article for Intellectual Content: Hellige, Seehusen, Rohn, Stadler

Category 3

(a) Final Approval of the Completed Article: Kottmeier, Hellige, Seehusen, Helweg, Rohn, Stadler

CONFLICT OF INTEREST

The authors confirm that there are no known conflicts of interest associated with this publication and there has been no significant financial support for this work that could have influenced its outcome.

NOTE

* Ethic approval statement: The research horses in this study underwent high-field MRI under general anesthesia and were euthanized due to a different study, which was approved by the animal welfare officer of the University of Veterinary Medicine Hannover, Foundation, Germany and the ethics committee of the responsible German federal state authority in accordance with the German Animal Welfare Law (Lower Saxony State Office for Consumer Protection and Food Safety, 33.9-42502-02-08/1622).

ORCID

Maren Hellige https://orcid.org/0000-0003-0549-2983

REFERENCES

1. Blunden A, Dyson SJ, Murray R, Schramme M. Histopathology in horses with chronic palmar foot pain and age-matched controls. Part 1: navicular bone and related structures. *Equine Vet J*. 2006;35:15-22. https://doi.org/10.2746/042516406775374298
2. Dyson SJ, Pool R, Blunden T, Murray R. The distal sesamoidean impar ligament: comparison between its appearance on magnetic resonance imaging and histology of the axial third of the ligament. *Equine Vet J*. 2010;42:332-339. https://doi.org/10.1111/j.2042-3306.2010.00068.x
3. Busoni V, Heimann M, Trenteseaux J, Snaps F, Dondelinger RF. Magnetic resonance imaging findings in the equine deep digital flexor tendon and distal sesamoid bone in advanced navicular disease—an ex vivo study. *Vet Radiol Ultrasound*. 2005;46:279-286. https://doi.org/10.1111/j.1740-8261.2005.00051.x
4. Murray R, Dyson SJ, Branch M, Schramme M. Validation of magnetic resonance imaging use in equine limbs. *Clin Tech Equine Pract*. 2007;6:26-36. https://doi.org/10.1053/j.ctep.2006.11.003
5. Murray R, Mair TS, Sherlock CE, Blunden A. Comparison of high-field and low-field magnetic resonance images of cadaver limbs of horses. *Vet Rec*. 2009;165:281-288.
6. Dyson SJ, Blunden T, Murray R. Comparison between magnetic resonance imaging and histological findings in the navicular bone of horses with foot pain. *Equine Vet J*. 2012;44:692-698. https://doi.org/10.1111/j.2042-3306.2012.00565.x
7. Murray R, Blunden T, Schramme M, Dyson SJ. How does magnetic resonance imaging represent histologic findings in the equine digit. *Vet Radiol Ultrasound*. 2006;47:17-31. https://doi.org/10.1111/j.1740-8261.2005.00101.x
8. Murray R, Schramme M, Dyson SJ, Branch M, Blunden T. Magnetic resonance imaging characteristics of the foot in horses with palmar foot pain and control horses. *Vet Radiol Ultrasound*. 2006;47:1-16. https://doi.org/10.1111/j.17408261.2005.00100.x
9. Cotten A, Delfaut E, Demondion X, et al. MR imaging of the knee at 0.2 and 1.5 T: correlation with surgery. *AJR Am J Roentgenol*. 2000;174:1093-1097. https://doi.org/10.2214/ajr.174.4.1741093
10. Schild H. Clinical highfield MR. *Fortschr Röntgenstr*. 2005;177:621-631. https://doi.org/10.1055/s-2005-858048
11. Wright IM, Kidd L, Thorp BH. Gross, histological and histomorphometric features of the navicular bone and related structures in the horse. *Equine Vet J*. 1998;30:220-234. https://doi.org/10.1111/j.2042-3306.1998.tb04491.x
12. Schramme M, Murray R, Blunden A, Dyson SJ. A comparison between MRI, pathology and radiology in 34 limbs with navicular syndrome and 25 control limbs. *Proc Am As equine Practnrs*. 2005;51:348-358.
13. Schramme M, Kerekes Z, Hunter S, Nagy K, Pease A. Improved identification of the palmar fibrocartilage of the navicular bone with saline magnetic resonance bursography. *Vet Radiol Ultrasound*. 2009;50:606-614. https://doi.org/10.1111/j.1740-8261.2009.01590.x
14. Graichen H, Jakob J, von Eisenhart-Rothe R, Englmeier K, Reiser M, Eckstein F. Validation of cartilage volume and thickness measurements in the human shoulder with quantitative magnetic resonance imaging. *Osteoarthr Cartilage*. 2003;11:475-482. https://doi.org/10.1016/S1063-4584(03)00077-3
15. Murray R, Branch M, Tranquille C, Woods S. Validation of magnetic resonance imaging of equine articular cartilage and subchondral bone thickness. *Am J Vet Res*. 2005;66:1999-2005. https://doi.org/10.2460/ajvr.2005.66.1999
16. Porter EG, Winter MD, Sheppard BJ, Berry CR, Hernandez JA. Correlation of articular cartilage thickness measurements made with magnetic resonance imaging, magnetic resonance arthrography, and computed tomographic arthrography with gross articular cartilage thickness in the equine metacarpophalangeal joint. *Vet Radiol Ultrasound*. 2016;57:515-525. https://doi.org/10.1111/vru.12390

17. Böck P. *Romeis mikroskopische technik*. Munich, Germany: Urban & Schwarzenberg; 2010.
18. Altman DG, *Practical statistic for medical research*. London, England: Chapman and Hall; 1991.
19. Yorke EH, Judy CE, Saveraid TC, McGowan CP, Caldwell FJ. Distal border fragments of the equine navicular bone: association between magnetic resonance imaging characteristics and clinical lameness. *Vet Radiol Ultrasound*. 2014;55:35-44. https://doi.org/10.1111/vru.12082
20. Hertsch BW, Steffen D. Comparative radiological and pathomorphological examinations of navicular bones with special attention being given to the sesamoidian canals—a contribution to the diagnosis of navicular diseases. *Dt Tieraerztl Wochenschr*. 1986;93:353-359.
21. Eckstein F, Sittek H, Milz S, et al. The potential of magnetic resonance imaging (MRI) for quantifying articular cartilage thickness—a methodological study. *Clin Biomech*. 1995;10:434-440. https://doi.org/10.1016/0268-0033(95)00013-1
22. McGibbon CA, Dupuy DE, Palmer WE, Krebs DE. Cartilage and subchondral bone thickness distribution with MR imaging. *Acad Radiol*. 1998;5:20-25. https://doi.org/10.1016/S1076-6332(98)80007-X
23. McGibbon CA, Bencardino J, Palmer WE. Subchondral bone and cartilage thickness from MRI: effects of chemical-shift artifact. *Mag Res Mat in Physics, Biology and Med*. 2003;16:1-9. https://doi.org/10.1007./s10334-003-0001-0

How to cite this article: Kottmeier LK, Seehusen F, Helweg M, Rohn K, Stadler P, Hellige M. High-field (3 Tesla) MRI of the navicular apparatus of sound horses shows good agreement to histopathology. *Vet Radiol Ultrasound*. 2020;61:48–57. https://doi.org/10.1111/vru.12825